Vol. 40 (2009) ACTA PHYSICA POLONICA B No 3

THE PYGMY DIPOLE RESONANCE IN THE NEUTRON-RICH NUCLEUS ^{68}Ni*

A. Bracco[a,b], O. Wieland[b]

[a]Dipartimento di Fisica, Universitá di Milano
via Celoria 16, 20133 Milano, Italy

[b]INFN Sez. di Milano, via Celoria 16, 20133 Milano, Italy

(Received December 30, 2008)

A search of the pygmy resonance in ^{68}Ni was made using the virtual photon technique. The experiment was carried out using the radioactive beam ^{68}Ni at 600 AMeV impinging on a Au target. The ^{68}Ni beam, produced at GSI with fragmentation of ^{86}Kr at 900 AMeV on a ^{9}Be target, was separated by the Fragment Separator and the gamma-rays produced at the interaction with the Au target were detected with the RISING set-up including also the HECTOR array. The measured gamma-ray spectra show a peak centered at approximately 11 MeV, whose intensity can be explained in term of an enhanced strength of the dipole response function (pygmy resonance). A pygmy structure of this type was also predicted by different models for this unstable neutron rich nucleus.

PACS numbers: 24.30.Cz, 24.10.Pa, 24.60.Dr, 27.60.+j

1. Introduction

Giant resonances are basic building blocks of nuclear structure. Because they dominate the nuclear response at low excitation energies, investigations of their main features such as centroid and widths have been carried out for many years in experimental nuclear physics. In the case of the simplest mode, the giant dipole resonance (GDR) a reasonable knowledge of its systematic features has been achieved. However, it is not generally known its fine structure which carries unique information on the underline nature of the mode and on the decay mechanisms. A very interesting long standing question is the nature of the so-called electric pygmy dipole resonance close to the neutron threshold in medium-to-heavy nuclei. It is predicted to result from

* Presented at the Zakopane Conference on Nuclear Physics, September 1–7, 2008, Zakopane, Poland.

a neutron excess density vibration relative to the $N \approx Z$ core. This mechanism interpreted the sizable low-lying E1 strength in very light neutron-rich nuclei. A good understanding of the properties of soft E1 modes (or pygmy) is important particularly in connection with exotic neutron rich nuclei. In fact, this allows to test predictions showing that the structural features of the GDR changes for extreme neutron-to-proton ratios. Furthermore, the presence of a resonance of E1 character close to particle threshold has important astrophysical implications because it considerably modifies the thermal equilibrium of (γ, n) and (n, γ) reactions in explosive nucleosyntesis scenarios [1]. A powerful tool to study the low lying E1 strength of unstable neutron rich nuclei is the scattering of high-energy radioactive beams in inverse kinematics. At beam energies of several hundred MeV/nucleon, the rapidly varying electromagnetic field of a high Z target experienced by the fast moving projectile, generates dipole transitions with relatively large cross sections up to excitation energies of the order of 20 MeV and thus opens the possibility of studying the dipole response of exotic nuclei. So far, experimental information on the E1 response in unstable nuclei is rather limited and the existing results are based on neutron breakup measurements [2–4]. A complementary approach is the virtual-photon-scattering method so far employed to study ^{20}O up to excitation energy of 7 MeV [5]. Here a report is given of the first measurement made for ^{68}Ni that uses the virtual-photon-scattering at much higher energy than that of ^{20}O in order to excite with the Coulomb field the region well above the nucleon binding energy. An important point is also that at this bombarding energy the excitation of vibrations of electric dipole character is dominating over other excitation modes [6]. The unstable nucleus ^{68}Ni represents a good case to search for pygmy structures being this nucleus located in the middle of the long isotopic Ni chain having at the extremes the doubly magic ^{56}Ni and ^{78}Ni. Furthermore, it is experimentally accessible with the present radioactive beam facilities. In addition, different theoretical predictions on the pygmy dipole strength are available for this mass region [7–9].

2. The experiment

The experimental method consists in the scattering of a high energy radioactive beam on a high Z target and in detecting gamma-rays in coincidence with the scattered particles at angles smaller than that corresponding to the grazing collision. A schematic drawing of the experimental set up is shown in Fig. 1.

The radioactive ^{68}Ni beam was produced by fragmentation of a primary ^{86}Kr beam delivered by the SIS synchrotron at GSI at 900 MeV/u and focused on a Be target. The ^{68}Ni ions were selected and transported with

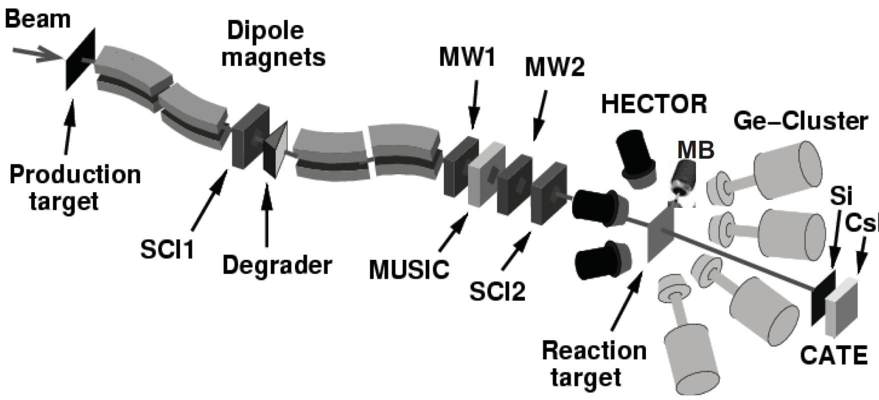

Fig. 1. A schematic view of the experimental set-up used for the experiment. The different gamma detectors are indicated with HECTOR (the BaF_2 scintillator detectors) MB (the HPGe detectors of the miniball array) and Ge-clusters (the HPGe of Euroball). The particle detectors before the target (gas counters and scintilators) are used to identify the incident particle while the CATE calorimeter is used to identify the reaction products.

the Fragment Separator FRS. The settings of the FRS were chosen to accept secondary fragments with a magnetic rigidity corresponding to a certain mass-over-charge ratio and that provided a beam cocktail containing in large fraction ^{68}Ni ions. The different nuclei contained in the secondary beam were identified uniquely according to their nuclear charge and mass number on an event-by-event basis. The ^{68}Ni ions constitute the most intense component (33% of the beam cocktail) impinging on the Au target (2 g/cm^2 thick). The particle identification after the Au target was performed using the calorimeter (CATE) [10] placed at 0°. This calorimeter consisted of nine thin position sensitive Si detectors placed in front of four 6 cm thick CsI scintillator detectors, arranged symmetrically with respect to the beam direction. The opening angle θ of the calorimeter CATE was $\pm 2.0°$, which is much larger than the grazing angle of this reaction. The grazing angle, corresponding to the maximum angle at which the interaction is strongly dominated by the Coulomb interaction is in this case equal to 0.43°. At larger angles the contribution of hadronic interaction becomes more important and therefore also other multipoles can be excited. The total energy and energy loss correlation of events in the CATE calorimeter corresponding to ^{68}Ni ions were measured with a FWHM which was found to be approximately 1%. Therefore the present resolution is sufficient to discriminate between different masses of the outgoing nuclei. The γ-ray emission at the target location was measured using a specific configuration of the RISING set-up [11]. Gamma rays were detected at different angles, at 16°, 33° and 36° with the 15 HPGe clusters of the RISING array, at 51° and 88° with 7 HPGe segmented clusters of the Miniball array and at 88° and 142° with 8 BaF_2 of the HECTOR array [12].

The good timing properties of the BaF_2 detectors were exploited to discriminate against gamma events originating at different locations along the beam line, using the time of flight measurement. This is illustrated in Figs. 2 and 3. The energy spectra of BaF_2 detectors are therefore characterized by

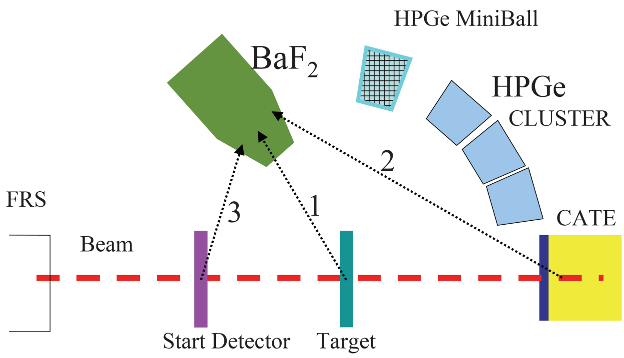

Fig. 2. A schematic drawing of a section of the experimental set up illustrating the different sources of gamma rays that are seen by the gamma detectors. With 1 are indicated the events at the target, with 2 the events at the CATE calorimeter, with 3 the events at the start scintillator detector.

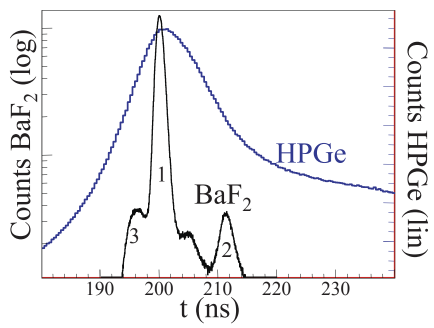

Fig. 3. Comparison of the time spectrum measured with the BaF_2 scintillator detectors with that measured with HpGe detectors. The different components of the time spectrum of BaF_2 are indicated with different numbers (the same used in Fig. 2). With 1 are indicated the events at the target, with 2 the events at the CATE calorimeter, with 3 the events at the start scintillator detector.

a much smaller background, particularly at low energy, in comparison with the HPGe detectors of the RISING set up. Conversely, the latter, having a much better energy resolution have allowed also to measure the B(E2) of the first 2^+ state. This is discussed in the following section.

3. The measurement of the low-lying quadrupole states

The study of the low-lying E2 strength distribution in ^{68}Ni and in other nickel isotopes has been a topic much investigated in recent years because the fragmentation of the low-lying quadrupole strength is sensitive to the size of the $N = 40$ gap. The doubly magic character of ^{68}Ni was suggested in the early 1980's and tested experimentally with a Coulomb excitation experiment performed at GANIL using a ^{68}Ni beam at 66 MeV/nucleon [13]. The proton number $Z = 28$ in the nickel isotopes is magic. In the neutron, the sizable energy gap at $N = 40$ separates the pf spherical shell from the $g_{9/2}$.

In the present experiment it was possible to confirm the results obtained in Ref. [13]. In fact, the low energy part of the gamma-ray spectrum measured with HPGe detectors shows the presence of the peak corresponding to the transition from the well known first 2^+ state of ^{68}Ni, as it can be seen in Fig. 4. The B(E2) strength measured for the transition at 2.033 MeV is found in this case to be 250 ± 100 e^2fm^4 in good agreement with the value of

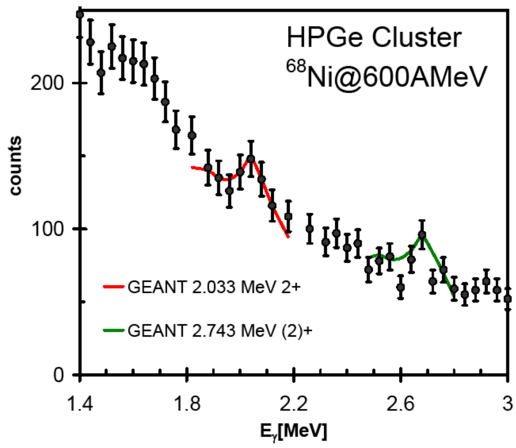

Fig. 4. Spectrum of gamma-rays measured for ^{68}Ni with the HPGe detectors. The results of a simulation with GEANT of the response function including the Doppler broadening effect are shown with the continuous lines overlying the peak structures.

the measurement at 66 MeV/nucleon equal to $255 \pm 60\ e^2\mathrm{fm}^4$. In addition, in the present case there is an indication, although rather weak, of a possible excitation of the second 2^+ state at 2.743 MeV, state seen in beta-decay [14] and transfer reaction [15] experiments.

4. The measurement of the pygmy dipole states

The γ-ray energy spectra for the ^{67}Ni and ^{68}Ni nuclei measured with the HPGe Euroball detectors are shown in the lower panels of Fig. 5. The two Ni isotopes are very well separated as illustrated in the top part of the same figure and are produced with different intensities, being that of ^{68}Ni the largest.

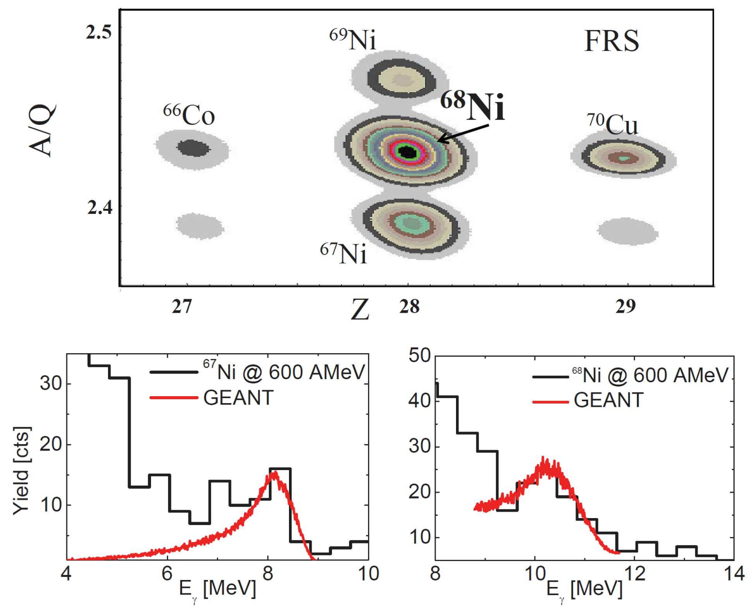

Fig. 5. In the upper panel the composition of the beam impinging on the Au target as selected with the fragment separator is shown. The A/Q versus Z plot of the ions used as a secondary beam is given and the arrow indicates the ^{68}Ni nuclei. In the bottom panels two gamma-ray spectra measured with the Euroball HPGe cluster detectors are shown. The spectrum of the left panel corresponds to the selection of ^{67}Ni as ingoing and outgoing particles and similarly the one on the right panel corresponds to the selection of ^{68}Ni. The continuous lines superimposed to the peak structures in ^{67}Ni and ^{68}Ni are GEANT simulations of the response of the detection system for monochromatic γ lines with $E_\gamma = 9, 11$ MeV, respectively.

To verify if the structures after the part of the spectrum with exponential shape are due to projectile emission, GEANT [17] simulations of the detector response at 9 and 11 MeV were made. These simulations are shown with the continuous lines in the lower panels of Fig. 5. At difference with the ^{68}Ni nucleus, in the case of ^{67}Ni the peaked structure is at an energy 2 MeV lower, reflecting the fact that also the neutron binding energy is 2 MeV lower, and is distributed over a wider energy interval. Similar structures were measured with the BaF_2 detectors. Since the BaF_2 scintillators are characterized by a better timing (see Figs. 2 and 3) it was possible for these detectors to make a better rejection of the background, important point for the extraction of the value of the E1 strength. In addition, in the case of the BaF_2 detectors it was possible to reproduce the exponential part of the spectrum with statistical model calculations (see Ref. [16]). This exponential part was then subtracted from the spectrum in order to extract the cross section for the gamma-decay from the pygmy.

In Fig. 6 (right panel) the cross section for the gamma decay of ^{68}Ni at $E_\gamma > 7$ MeV measured with the BaF_2 detectors is shown. The measured cross section is compared with predictions obtained making different assumptions for the E1 strength function. In particular, the ingredients of

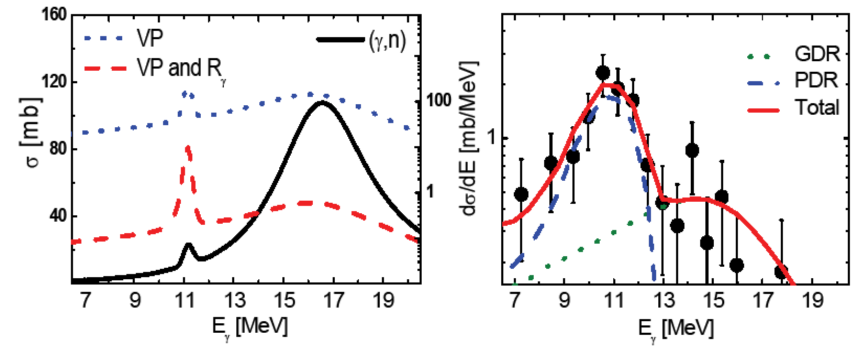

Fig. 6. In the left panel the ^{68}Ni photoabsorption strength is shown with a fully drawn line (scale on the left). The resulting differential cross section after applying the equivalent photon method is shown with a dotted line (scale on the right). A dashed line (scale on the left) shows the effect of including additionally the branching ratio. In the right panel the measured cross section with the BaF_2 detectors is shown with circles (the statistical contribution was subtracted). The corresponding predictions (folded with the detector response function) are shown with lines. The long-dashed line shows the prediction when only a PDR strength is considered, the short-dashed line corresponds to the standard GDR strength without a pygmy component, and the full drawn-line is the sum of the two calculations.

the calculations are shown in the left panel of Fig. 6. In this panel an electric dipole response function with a small peak at 11 MeV with 5% of the energy weighted sum rule (EWSR) strength is shown. The corresponding function when modified by the virtual photon number is shown with the dotted line. The additional and very important effect of the gamma branching ratio R_γ is displayed with dashed line curve. This latter contribution depends on the nuclear level density. For the present calculation the adopted level density is based on Shell Model Monte Carlo calculations ([18]). Using this level density the total gamma branching ratio is found to vary from 0.4% to 4% going from the region of the GDR to the region of the pygmy resonance. For the proper comparison of the calculation to the data the detector response function was folded. A more detailed description of these calculations is in reference [16].

There is a remarkable agreement of the calculated cross section with the data (without any normalization factor) both in size and shape when one assumes an electric dipole strength function with 5% of EWSR strength at 11 MeV (the corresponding $B(\mathrm{E1})$ value being 1.2 $e^2\mathrm{fm}^2$). Presently two different predictions are available for the pygmy resonance in Ni isotopes, one based on relativistic random phase approximation ([7]) and the other based on quasi particle relativistic random phase [8] both predicting at 9–10 MeV a pygmy structure with a EWSR strength of 4% and 10%, respectively. The present data can be fitted with 9% of the EWSR strength if one uses as level density a simple extrapolation from stable nuclei (≈ 5 times larger than the one used in Fig. 6).

5. Conclusions

The first experimental search of the pygmy resonance in the neutron rich ^{68}Ni nucleus using the the virtual photon scattering technique is here presented. The RISING set up and a beam at 600 MeV/nucleon impinging on a Au target were employed. Evidence is found for the presence of a pygmy component in the E1 response energetically located below the GDR and centered at ≈ 11 MeV with $\approx 5\%$ of the EWSR strength. This result is in rather good agreement with theoretical predictions and provides a relevant information which could be related to neutron skin and nuclear symmetry energy ([2]). An analysis to extract the neutron skin is planned.

In the near future measurements of the pygmy in the ^{26}Ne nucleus are planned with an improved RISING set-up.

The present result opens interesting future perspectives for investigations of nuclear structure with relativistic beams using more intense radioactive beams and better performing instrumentation for gamma-ray detection such as AGATA and GRETA. In fact, it will be important for the understanding of the neutron skin in nuclei far from stability to measure more in detail and more systematically the structure of the electric dipole response in an energy interval larger than that of the present experiment. This requires higher energy resolution and efficiency for the gamma detectors and also more intense beams of nuclei further away from stability as those which will become available at FAIR.

We would like to thank all the collaborators taking part in this experiments. They are F. Camera, G. Benzoni, N. Blasi, S. Brambilla, F.C.L. Crespi, S. Leoni, B. Million, R. Nicolini, A. Maj, P. Bednarczyk, J. Grebosz, M. Kmiecik, W. Meczynski, J. Styczen, T. Aumann, A. Banu, T. Beck, F. Becker, L. Caceres, P. Doornenbal, H. Emling, J. Gerl, H. Geissel, M. Gorska, O. Kavatsyuk, M. Kavatsyuk, I. Kojouharov, N. Kurz, R. Lozeva, N. Saito, T. Saito, H. Schaffner, H.J. Wollersheim, J. Jolie, P. Reiter, N. Warr, G. de Angelis, A. Gadea, D. Napoli, S. Lenzi, S. Lunardi, D. Balabanski, G. Lo Bianco, C. Petrache, A. Saltarelli, M. Castoldi, A. Zucchiatti, J. Walker, A. Bürger. This work was partially supported by the Italian National Institute of Nuclear Physiscs (INFN) and by the Polish Commitee for Scientific Research (KBN Grant No. 1 P03B 030 30).

REFERENCES

[1] S. Goriely, *Phys. Lett.* **B436**, 10 (1998); S. Goriely, E. Khan, *Nucl. Phys.* **A706**, 217 (2002).
[2] A. Klimkiewicz *et al.*, *Phys. Rev.* **C76**, 051603 (2007).
[3] A. Leistenschneider *et al.*, *Phys. Rev. Lett.* **86**, 5442 (2001).
[4] P. Adrich *et al.*, *Phys. Rev. Lett.* **95**, 132501 (2005).
[5] E. Tryggestad *et al.*, *Phys. Lett.* **B541**, 52 (2002).
[6] T. Aumann, *Eur. Phys. J.* **A26**, 441 (2005).
[7] D. Vretnar *et al.*, *Nucl. Phys.* **A692**, 496 (2001).
[8] L. Cao, Z. Ma, *Mod. Phys. Lett.* **A19**, 2845 (2004).
[9] N. Paar *et al.*, *Rep. Prog. Phys.* **70**, 691 (2007).
[10] R. Lozeva *et al.*, *Nucl. Instrum. Methods* **A562**, 298 (2006).
[11] H.J. Wollersheim *et al.*, *Nucl. Instrum. Methods* **A537**, 637 (2005).
[12] A. Bracco *et al.*, *Rev. Mod. Phys. Lett.* **33**, 2479 (2007).
[13] O. Sorlin *et al.*, *Phys. Rev. Lett.* **99**, 092501 (2002).
[14] W.F. Mueller *et al.*, *Phys. Rev.* **C61**, 054308 (2000).
[15] M. Girod *et al.*, *Phys. Rev.* **C37**, 2600 (1988).
[16] O. Wieland *et al.*, submitted to *Phys. Rev. Lett.*
[17] R. Brun *et al.*, CERN Report No. CERN-DD/EE/84-1.
[18] Y. Alhassid *et al.*, *Phys. Rev. Lett.* **99**, 162504 (2007).